



**Biomaterials
Science**

**Injectable Hydrogel Mediated Delivery of Gene-Engineered
Adipose-Derived Stem Cells for Enhanced Osteoarthritis
Treatment**

Journal:	<i>Biomaterials Science</i>
Manuscript ID	BM-ART-07-2021-001122.R1
Article Type:	Paper
Date Submitted by the Author:	23-Sep-2021
Complete List of Authors:	<p>Yu, Wei; Shanghai Jiao Tong University, Engineering Research Center of Cell & Therapeutic Antibody, Ministry of Education, and School of Pharmacy</p> <p>Hu, Bin; Shanghai Jiao Tong University, Engineering Research Center of Cell & Therapeutic Antibody, Ministry of Education, and School of Pharmacy</p> <p>Boakye-Yiadom, Kofi Oti ; Shanghai Jiao Tong University, Engineering Research Center of Cell & Therapeutic Antibody, Ministry of Education, and School of Pharmacy</p> <p>Ho, William; New Jersey Institute of Technology, Department of Chemical and Materials Engineering</p> <p>Chen, Qijing; Shanghai Jiao Tong University, Engineering Research Center of Cell & Therapeutic Antibody, Ministry of Education, and School of Pharmacy</p> <p>Xu, Xiaoyang; New Jersey Institute of Technology, Department of Chemical and Materials Engineering</p> <p>Zhang, Xue-Qing; Shanghai Jiao Tong University, Engineering Research Center of Cell & Therapeutic Antibody, Ministry of Education, and School of Pharmacy</p>

SCHOLARONE™
Manuscripts

ARTICLE

Injectable Hydrogel Mediated Delivery of Gene-Engineered Adipose-Derived Stem Cells for Enhanced Osteoarthritis Treatment

Received 00th January 20xx,
Accepted 00th January 20xx

Wei Yu,^a Bin Hu,^a Kofi Oti Boakye-Yiadom,^a William Ho,^b Qijing Chen,^a Xiaoyang Xu,^{*b} and Xue-Qing Zhang^{*a}

DOI: 10.1039/x0xx00000x

Osteoarthritis (OA), a chronic and degenerative joint disease, remains a challenge in treatment due to the lack of disease-modifying therapies. As a promising therapeutic agent, adipose-derived stem cells (ADSCs) perform an effective anti-inflammatory and chondroprotective paracrine effect that could be enhanced by genetic modification. Unfortunately, direct cell delivery without matrix support often results in poor viability of therapeutic cells. Herein, a hydrogel implant approach that enabled intra-articular delivery of gene-engineered ADSCs was developed for improved therapeutic outcomes in a surgically induced rat OA model. An injectable extracellular matrix (ECM)-mimicking hydrogel was prepared as the carrier for cell delivery, providing a favorable micro-environment for ADSCs spreading and proliferation. The ECM-mimicking hydrogel could reduce cell death during and post-injection. Additionally, ADSCs were genetically modified to overexpress transforming growth factor- β 1 (TGF- β 1), one of the paracrine factors that exert an anti-inflammatory and pro-anabolic effect. The gene-engineered ADSCs overexpressing TGF- β 1 (T-ADSCs) perform an enhanced paracrine effect on OA-like chondrocytes, which effectively decreases the expression of tumor necrosis factor- α and increases the expression of collagen II and aggrecan. In the surgically induced rat OA model, intra-articular injection of T-ADSCs-loaded hydrogel remarkably reduced the cartilage degeneration, joint inflammation, and loss of subchondral bone. Taken together, this study provides a potential biomaterial strategy for enhanced OA treatment by delivering the gene-engineered ADSCs within an ECM-mimicking hydrogel.

Introduction

Osteoarthritis (OA) is a chronic and degenerative joint disease characterized by articular cartilage degeneration, synovitis, and subchondral bone remodeling.¹ It impairs an estimated 10% of men and 18% of women aged over 60 in the world.^{2,3} However, the lack of effective disease-modifying therapies for its treatment results in the progressive development of OA, drastically affecting the life quality of patients.⁴

As a potential therapeutic agent, adipose-derived stem cells (ADSCs) have recently been extensively studied to slow down the progress of articular cartilage destruction and circumvent inflammation.⁵ They perform a paracrine function by secreting large amounts of anti-inflammatory mediators and chondroprotective molecules.⁶⁻⁸ Transforming growth factor- β 1 (TGF- β 1) is an important paracrine factor secreted by ADSCs.⁹

Previous studies have confirmed that TGF- β 1 facilitated the production of ECM proteins and blocked the stimulation of interleukin 1 beta (IL-1 β) on chondrocytes.^{10,11} Therefore, it exerts chondroprotective effects and prevents the cartilage from further damage. A recent finding also suggested that TGF- β 1 could exert an anti-inflammatory effect by inducing an M2 macrophage-dominant micro-environment in the OA-affected joint.¹² Herein, the ADSCs were genetically engineered to continuously overexpress TGF- β 1 to further enhance its chondroprotective and anti-inflammatory effects for OA treatment.

Delivering cells into the joint through intra-articular injection is a fairly common practice for ADSCs administration. Unfortunately, direct cell injection without matrix support often results in significantly declined cell viability.¹³⁻¹⁵ Hydrogel is the three-dimensional hydrophilic polymeric network with reticulated structure, high water content, and adjustable mechanical properties. Therefore, hydrogels provide structural support for cells and facilitate the transport of oxygen, nutrient, waste, and soluble factors.^{16,17} The injectable hydrogel has recently emerged as a promising carrier for cell delivery because it provides a minimally invasive method to deliver cells into tissues.¹⁸⁻²¹ The injectable ECM-mimicking hydrogels with cell adhesion sites are especially attractive due to their capacities to promote cell spreading and proliferation.¹⁶ However, the therapeutic effects of gene-engineered ADSCs

^a Engineering Research Center of Cell & Therapeutic Antibody, Ministry of Education, and School of Pharmacy, Shanghai Jiao Tong University, Shanghai 200240, P. R. China

E-mail: xueqingzhang@sjtu.edu.cn

^b Department of Chemical and Materials Engineering, New Jersey Institute of Technology, Newark, NJ 07102, USA

E-mail: xiaoyang@njit.edu

Electronic Supplementary Information (ESI) available: [details of any supplementary information available should be included here]. See DOI: 10.1039/x0xx00000x

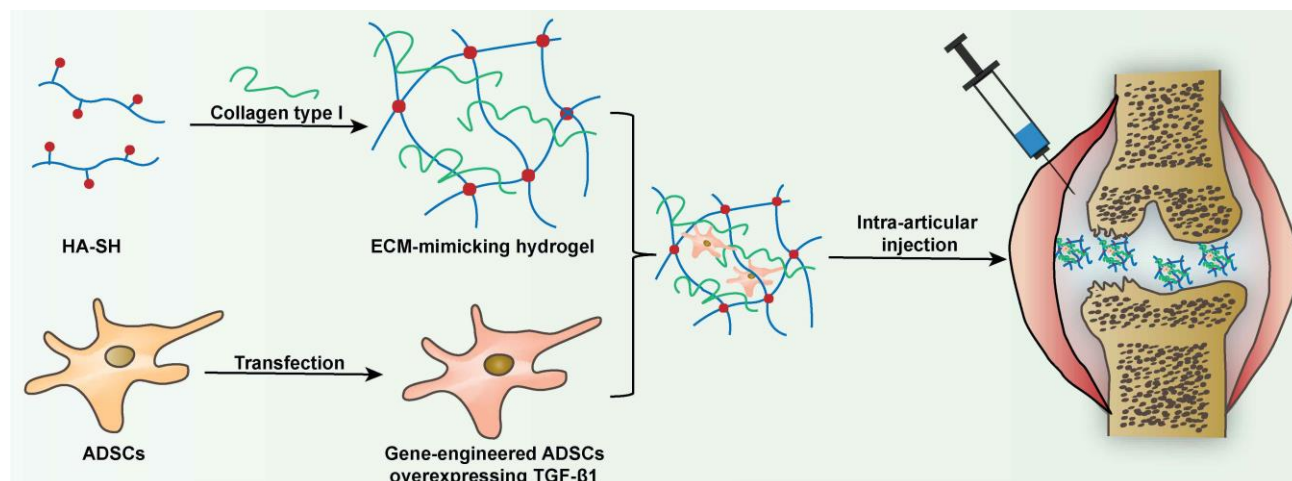


Fig. 1 A schematic demonstration of the experimental design. An injectable ECM-mimicking hydrogel was prepared via self-crosslinking of thiolated hyaluronic acid (HA-SH) and self-assembling of collagen type I (Col I). The gene-engineered ADSCs overexpressing TGF- β 1 were encapsulated in the prepared hydrogel and delivered into the knee joint of the rat OA model for OA treatment.

coupled with an injectable ECM-mimicking hydrogel for OA treatment has not yet been investigated.

Herein, we have developed an injectable ECM-mimicking hydrogel approach that facilitates minimally invasive delivery of ADSCs overexpressing TGF- β 1 (T-ADSCs) to improve the therapeutic outcomes of OA treatment (Fig. 1). The in situ formed hydrogel implant is degradable and biocompatible with tunable physical properties, which provides a favorable 3-dimensional (3D) environment for cell growth, leading to improved cell retention and survival and long-lasting expression of therapeutic protein TGF- β 1. *In vitro* 3D culture and cell injection experiments were conducted to evaluate the cytocompatibility and cell protection potential of the hydrogel. The ADSCs were transfected with plasmid encoding TGF- β 1 to overexpress TGF- β 1 protein. The paracrine protective effect of the T-ADSCs was evaluated in a co-culture system. The *in vivo* therapeutic effects of the developed combinatorial therapy were investigated through micro-computed tomography (micro-CT) and histological analysis. Noteworthy, this hydrogel-mediated drug delivery approach coupled with gene-engineered cell therapy could be easily tuned for other biomedical applications of interest, providing great potential for future clinical practices and treatments.

Materials and Methods

Materials

Hyaluronic acid (HA, Mw = 100 kDa) was purchased from Bloomage Freda Biopharm Co., Ltd. (Shandong, China). 1, 4-butanediol diacrylate, 4-amino-1-butanol, and 1-(3-aminopropyl)-4-methyl piperazine were purchased from Sigma-Aldrich (Shanghai, China). Other chemical reagents were purchased from Aladdin (Shanghai, China). Rat tail Col I was purchased from BD BioCoat. Dulbecco's modified Eagle medium/Ham's F-12 medium (DMEM/F12), fetal bovine serum

(FBS), penicillin (Pen), and streptomycin (Strep) were purchased from Gibco (Shanghai, China). CD90 and CD45 antibodies were purchased from BioLegend (San Diego, CA). Safranin O/Fast Green staining solution, hematoxylin, and eosin were purchased from Servicebio Technology Co., Ltd. (Wuhan, China).

Synthesis and characterization of thiolated hyaluronic acid (HA-SH)

HA-SH was synthesized according to a previously described method with slight modifications.²² Briefly, HA (1 g) was dissolved in deionized water (DI-H₂O, 100 mL) and the pH was adjusted to 5.5. N-(3-Dimethylaminopropyl)-N'-ethyl carbodiimide hydrochloride (1.22 g) was added to the resultant solution and this reaction process occurred for 30 mins. Subsequently, N-hydroxysuccinimide (0.73 g) and cysteamine hydrochloride (1.16 g) were added to the reaction mixture and the reaction process was sustained for another 4 h while adjusting the pH in the range of 4.75 ~ 5.0. The final reaction solution was transferred into dialysis tubes (3.5 kDa) and dialyzed against DI-H₂O (pH = 3.5) containing 0.1 M NaCl for 48 h and then another 24 h dialysis against DI-H₂O (pH = 3.5). The purified solution was lyophilized to yield the HA-SH polymer. ¹H NMR spectra of HA-SH and HA were recorded on an Agilent 400 MHz NMR spectrometer.

Preparation of the hydrogels

Either the Col I solution (1.3 mg mL⁻¹, 550 μ L) or 1 \times PBS (550 μ L) was used to dissolve a certain amount of HA-SH polymer. The pH of the solution was adjusted to 7.8 using 1 N NaOH, and a certain amount of 1 \times PBS was added to get a final volume of 600 μ L. Finally, the mixed solution was transferred into a cylindrical Teflon mold with different diameters (8 mm or 24 mm) to form the hydrogels.

Swelling test

The hydrogel disks (diameter = 8 mm, height = 1.5 mm) were incubated in PBS (7.4) for 24 h at 37 $^{\circ}$ C. The swollen hydrogels were accurately weighed (W_t) after the excess amount of water was removed from the washed gels (DI-H₂O, 3 \times washing) using a filter

paper. The hydrogel samples were lyophilized to determine the dried weight (W_0). The swelling ratio (Q_m) was calculated by comparing the initial weight (W_i) with the dried hydrogel weight (W_0) as shown below ($n = 3$):

$$Q_m = W_i/W_0 \quad (1)$$

Degradation test

The hydrogel disks (diameter = 8 mm, height = 1.5 mm) were lyophilized and the initial weight (W_0) was recorded. The dried hydrogel disks were immersed in PBS (7.4) with or without 50 U mL⁻¹ hyaluronidases (Yeasen, China) and shaken at a speed of 200 rpm/min at 37 °C in a mechanical shaker (Zhichu ZQZY-CF, China). At pre-established time points, the hydrogel disks were removed from incubation, washed with DI-H₂O, and lyophilized to obtain the weight of dried gels (W_t). Hydrogel weight loss was calculated according to the formula below ($n = 3$):

$$\text{Weight loss (\%)} = [(W_0 - W_t)/W_0] \times 100\% \quad (2)$$

Rheological test of the hydrogels

Kinexus ultra+ rheometer (Malvern, UK) was used to test the mechanical properties of hydrogels. The prepared hydrogels were placed on a 25 mm parallel plate with a gap of 500~750 μm to run the stress and frequency sweeps under a controlled stress of 1 Pa ($n = 3$) at 37 °C. The shear-thinning property of HA-Col hydrogel was characterized by measuring linear viscosity (η) under a time sweep mode at 37 °C.

Isolation and characterization of ADSCs

All experiments involving primary cell extraction were conducted under approved animal welfare protocols (Institutional Animal Care and Use Committee, Shanghai Jiao Tong University). ADSCs were isolated from inguinal regions of the adipose tissue of the rats.²³ The morphology of ADSCs was imaged by an inverted phase microscope after staining (Olympus). Flow cytometry (BD Fortessa) was used to identify the surface biomarkers of ADSCs. The differentiation potential of ADSCs was evaluated in adipogenic, osteogenic, and chondrogenic induced culture media (Saiye Biotechnology, China). ADSCs passaged for the third time were used in the following experiments.

3D culture of ADSCs

ADSCs suspension was mixed with HA-SH and Col I solutions to get a final concentration of 1×10^6 cells mL⁻¹ cell-hydrogel constructs. They were transferred into a 24-well plate and DMEM/F12 supplemented with 10% FBS and 1% Pen/Strep were added. At days 1, 3 and 5, the ADSCs morphology in the different cell-hydrogel constructs was imaged using an inverted phase microscope. The viability of ADSCs encapsulated in hydrogel was evaluated by live/dead staining (Dalian Meilun, China), the cell-hydrogel construct was harvested after 3 days of 3D culture and stained with 2×10^{-3} M Calcein acetoxymethyl ester (Calcein AM) and 8×10^{-3} M pyridine iodide (PI) in PBS for 30 mins. Then it was imaged using a confocal microscope (Leica).

Evaluation of the protective effect of 2-HA-Col hydrogel on cells

The cell-hydrogel construct was transferred into a syringe which was then excluded from a 25-gauge needle. The confocal dish was used to collect the excluded cell-hydrogel construct. A small amount of medium was added and incubated at 37 °C with 5% CO₂ for 1 h, followed by live/dead staining. Fluorescence images were taken by a confocal microscope. ADSCs suspended in 1× PBS served as the control. The viability of cells in 2-HA-Col hydrogel was calculated using ImageJ software ($n = 3$).

SEM characterization

The sectional surface of dried 2-HA-Col hydrogel or cell-hydrogel construct harvested after 1 day of 3D culture was coated with a layer of 5 nm gold (EM ACE600, Leica). The microstructure of 2-HA-Col hydrogel or cell morphology in the 2-HA-Col hydrogel was observed by SEM (MIRA3, TESCAN). The average pore size of 2-HA-Col hydrogel was calculated using ImageJ software ($n = 3$).

Gene transfection

P2A, a cleavable 2A peptide sequence,²⁴ was cloned into the pcDNA3.1(+) plasmid between the enhanced green fluorescent protein (EGFP) gene and TGF-β1 gene (pEGFP-TGF-β1, GENEWIZ, China). Poly(β-amino ester) (PBAE) was synthesized and used as the pEGFP-TGF-β1 delivery carrier.²⁵ The optimal ratio of PBAE to pEGFP-TGF-β1 was determined by agarose gel retardation assay. The mean size and zeta potential of the PBAE/pEGFP-TGF-β1 nanocomplexes were determined by using a dynamic light scattering spectrophotometer (Malvern, UK). For cell transfection, ADSCs (6×10^4 cells per well) were seeded in a 24-well plate. After 12 h, the ADSCs were treated with serum-free DMEM/F12 containing different PBAE/pEGFP-TGF-β1 nanocomplexes (2 μg pEGFP-TGF-β1 for each well). The PBAE/pEGFP-TGF-β1 nanocomplexes were removed and replaced with a fresh culture medium after 4 h of incubation. The expression of EGFP in cells was imaged by a fluorescence microscope (Olympus), and the transfection efficiencies were determined by flow cytometry after 24 h of transfection ($n = 3$). Non-transfected ADSCs were used as controls.

Cell viability test

A Cell Counting Kit-8 (CCK-8) assay (Beyotime, China) was used to evaluate the toxicity of different nanocomplex formulations. ADSCs were seeded into 96 wells at a density of 5×10^3 per well for the cell toxicity assay and a density of 2×10^3 per well for the cell proliferation test. Cells were transfected (0.32 μg pEGFP-TGF-β1 for each well) as the method described above. At predetermined time points, the cell viability was examined according to the manufacturer's instruction ($n = 3$). Non-transfected ADSCs were used as controls.

Preparation and characterization of T-ADSCs

ADSCs (2.5×10^4 cells per well) were seeded in a 24-well plate. After 12 h, the cells were transfected using the optimal nanocomplex formulation. The expression of EGFP in cells was assessed using a fluorescence microscope, and the transfection efficiencies were determined by flow cytometry. The cell culture supernatant was collected at each defined time point and it was replaced with a fresh

medium every two days. ELISA (Neobioscience, China) test was performed to quantify the concentration of TGF- β 1 in culture supernatants of T-ADSCs ($n = 3$). The supernatants of non-transfected ADSCs were used as controls.

Co-culture of ADSCs and chondrocytes

Primary chondrocytes were isolated from the knee joint cartilage of the rats.²⁶ Chondrocytes were identified by immunocytochemistry of collagen type II (Col II).²⁷ Chondrocytes that were passaged for the first time were used in all experiments.

Chondrocytes (2.5×10^4 cells per well) were seeded in six-well plates or cell culture inserts (0.4 μ m pores, BD Falcon™), and ADSCs (2.5×10^4 cells per insert) were seeded in cell culture inserts, both containing DMEM/F12 supplemented with 10% FBS, 1% Pen/Strep. After 12 h, the ADSCs were transfected with PBAE/pEGFP-TGF- β 1 nanocomplexes. Then after another 12 h, the co-culture systems were established between T-ADSCs, ADSCs, or chondrocytes in cell culture inserts and chondrocytes in six-well plates as below: (1, Control) chondrocytes (well) and chondrocytes (insert); (2, IL-1 β) chondrocytes (well) and chondrocytes (insert); (3, IL-1 β +ADSCs) chondrocytes (well) and ADSCs (insert); (4, IL-1 β +T-ADSCs) chondrocytes (well) and T-ADSCs (insert). The control group was cultured in DMEM/F12 supplemented with 10% FBS, 1% Pen/Strep. On the other hand, the culture medium of other groups was supplemented with 10 ng mL⁻¹ IL-1 β (Neobioscience, China) to stimulate isolated chondrocytes to mimic OA chondrocytes.²⁸ After 3 days of co-culture, the total RNA of the chondrocytes in the well was extracted and analyzed using quantitative reverse transcription PCR (qRT-PCR). The primer sequences for the qRT-PCR are listed in Table S1. All the values were normalized and compared to GAPDH ($n = 3$).

Surgically induced rat OA model

Male Sprague-Dawley (SD) rats (180~200 g, 7 weeks old) were purchased from Shanghai SLAC Laboratory Animal Co., Ltd. The rats were housed in a specific pathogen-free environment in the animal center of Shanghai Jiao Tong University. All surgical and care procedures were reviewed and approved by the Institutional Animal Care and Use Committee (Shanghai Jiao Tong University).

1 week later, OA was surgically induced on the right knee of the rat by anterior cruciate ligament transection and partial medial meniscectomy (ACLT/MMx).²⁹ Briefly, the rats were anesthetized with 1% pentobarbital sodium (40 mg kg⁻¹). The right hindlimb was shaved and disinfected with iodophor. Two incisions (0.5~1 cm) were made with a #11 scalpel on the skin and joint capsule until the patella could be subluxated laterally, exposing the joint. The ACL was exposed and transected with microscissors, the anterior drawer test was conducted to confirm the transection. Subsequently, the medial meniscus was partially transected with a #11 blade and carefully taken out with tweezers. After the completion of the procedure, the patella was relocated. The joint capsule was closed with a 5-0 resorbable suture while the skin was closed with a 4-0 normal suture. After surgery, rats were given penicillin sodium to prevent surgery-associated infections.

4 weeks post-surgery, the rats were divided into 5 groups ($n = 5$ per group): PBS (40 μ L), ADSCs (2×10^5 cells in 40 μ L PBS), T-ADSCs (2×10^5 cells in 40 μ L PBS), Gel+ADSCs (2×10^5 cells in 40 μ L gel) and Gel+T-ADSCs (2×10^5 cells in 40 μ L gel). The rats treated with the sham surgery were used as control (Sham, $n = 5$). The T-ADSCs and cells-loaded hydrogel were prepared following the methods described above. Treatments were administered by intra-articular injection into the affected joint on the 4th and 6th week after surgery.

Quantitation of tumor necrosis factor-alpha (TNF- α) concentration in synovial fluid

Rats were sacrificed after 4 weeks of intra-articular injection. The joint cavity was flushed with 40 μ L of cold 1 \times PBS (pH=7.4), and about 20 μ L of diluted synovial fluid was carefully collected for each rat. The collected samples were centrifuged at 1×10^4 rpm min⁻¹ for 10 min and stored at -80 °C prior to ELISA analysis. TNF- α concentration in synovial fluid was determined by ELISA (Neobioscience, China).

Micro-CT scanning

The knee joints of three rats were randomly chosen from each group and imaged in a micro-computed tomographic scanner (VENUS micro-CT, PINGSENG, China). Scanning was performed using a 90 kV voltage and 0.07 mA current. 3D reconstruction of CT image datasets and regions of interest (ROI) analysis of trabecular bone were performed on an image processing software (VENUS, PINGSENG, China).

Histological analysis

The knee joints were decalcified in 10% ethylenediaminetetraacetic acid for 5 weeks and it was changed every two days. Decalcified bone tissues were embedded in paraffin wax, cut into 5 nm sections, and stained with hematoxylin/eosin (H&E), Safranin O (4% w/v) /Fast Green (0.1% w/v). Primary antibodies against Col II (Servicebio, 1:200) was used for immunohistochemical staining to observe the expression of Col II in cartilage. Cartilage lesions were graded by two blinded graders using a modified Mankin scales,³⁰ and the sections of synovial joint tissue were scored for three features, according to Krenn: inflammatory infiltrate, synovial stroma and lining cell hyperplasia.³¹

Statistical analysis

All values were presented as mean \pm standard deviation. Statistical comparison was analyzed via Student's *t*-test using GraphPad Prism 8. A *p*-value < 0.05 was considered statistically significant (*). **, ***, and **** represent $p < 0.01$, $p < 0.001$, and $p < 0.0001$. $p > 0.05$ was not significant (ns).

Results

Synthesis and characterization of HA-SH

The modification of HA resulted in the new resonant peaks in the ¹H NMR spectra at 2.52 ppm and 2.31 ppm (Fig. S1, Supporting Information), corresponding to the methylene

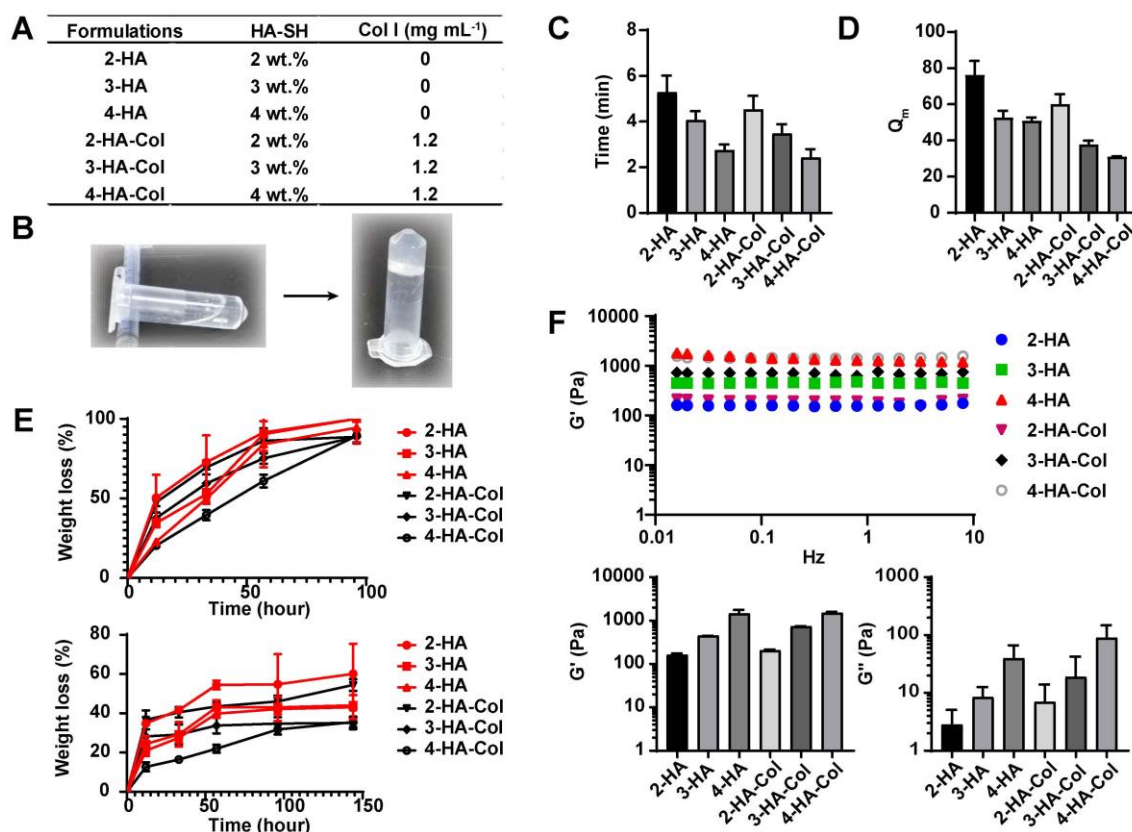


Fig. 2 Characterization of the different hydrogel formulations. A) Formulation of different hydrogels. B) The representative photographs of sol-to-gel transition of hydrogel. C) Time needed for sol-to-gel transition of the hydrogels. $n = 3$. D) Swelling ratio (Q_m) of various hydrogel formulations. $n = 3$. E) *In vitro* degradation of hydrogels in PBS with (top) or without (bottom) 50 U mL⁻¹ hyaluronidases at 37 °C. $n = 3$. F) Representative curves of storage modulus (G') of various hydrogel formulations (top). Statistics of G' and loss modulus (G'') of various hydrogel formulations (bottom). Rheological frequency sweep performed with the controlled stress of 1 Pa. $n = 3$. Data are presented as the mean \pm standard deviation ($n = 3$).

protons of $-\text{CH}_2\text{CH}_2\text{SH}$ groups.³² The amount of the thiol groups conjugated on HA backbone was 3.98×10^{-4} mol g⁻¹ determined by Ellman's assay.³³

Sol-to-gel transition

The hydrogel formulations were listed in Fig. 2A. The precursor solution of hydrogel turned into a gel adjusting its pH to 7.8 (Fig. 2B). Rapid sol-to-gel transitions were observed within 6 minutes for all the hydrogel formulations determined by an invert-flow test (Fig. 2C).³⁴

Swelling and degradation

The swelling ratio of HA hydrogels formed through the crosslinking of HA-SH reduced with the increase of HA-SH mass fraction, in the range of 50.2 to 76.2 (Fig. 2D). When Col I was incorporated into the HA hydrogels, the swelling ratio of hydrogels significantly decreased by 21.1%, 26.4, and 38.2% for hydrogels termed 2-HA-Col, 3-HA-Col, and 4-HA-Col, respectively. When incubated in PBS containing 50 U mL⁻¹ hyaluronidases, 2-HA was completely degraded in 4 days, and other hydrogels remained less than 12% of their weights (Fig. 2E). However, the hydrogels exhibited a much slower degradation rate in PBS, where only an approximate weight of 60% was degraded for the 2-HA hydrogel on day 6. And the

incorporation of Col I slowed down the degradation of the hydrogels in all cases.

Rheological properties

The hydrogel exhibited a linear viscoelastic behavior when the shear stress was in the range of 0.1 Pa to 10 Pa (Fig. S2), and the shear stress of 1 Pa was selected for subsequent sweeps. As shown in Fig. 2F, the storage modulus (G') and loss modulus (G'') of hydrogels were elevated with an increase in HA-SH mass fraction. The G' of the yielded HA hydrogels varied from 162.5 Pa to 1453.3 Pa. The addition of Col I further improved the G' and G'' values of hydrogels. The G' of 2-HA-Col, 3-HA-Col, and 4-HA-Col hydrogel increased by 27.0%, 63.8%, and 3.6%, respectively, when compared with their corresponding HA hydrogels. While no differences were observed in G'' before and after the addition of Col I. It is worth noting that the HA-Col hydrogel displayed a shear-thinning behavior that is desirable for its use to deliver cells through injection (Fig. S3, Supporting Information).³⁵ The viscosity of the hydrogel decreased from 137.2 Pa.s to 36.07 Pa.s with an increase in shear rate.

3D culture of ADSCs

ADSCs were isolated from rat inguinal adipose tissue. As shown in Fig. S4A, the isolated cells exhibited a fibroblast-like

morphology. Phenotypic analysis via flow cytometry indicated that the isolated cells were positive for mesenchymal stem cells marker CD90 and negative for hematopoietic lineage marker CD45 (Fig. S4B and S4C).³⁶ When cultured in the induced medium, the isolated cells differentiated toward the adipogenic, osteogenic, or chondrogenic lineage, showing the typical characteristics of ADSCs (Fig. S4D-F).³⁷

The ADSCs were encapsulated in hydrogels for 3D culture. ADSCs in 2-HA-Col and 3-HA-Col hydrogel started to spread and form protrusions at day 1 (Fig. 3A). However, cells in 4-HA-Col hydrogel maintained a spherical morphology without spreading over time. On days 3 and 5, the cells in 2-HA-Col and 3-HA-Col hydrogel matrix exhibited more elongated morphology and formed interconnected networks. Among the three hydrogels tested, the 2-HA-Col hydrogel provided considerable benefits through promoting cell spreading and proliferation as shown in

Fig. 3A. The live/dead staining of ADSCs after 3 days of culture in 2-HA-Col hydrogel demonstrated that most of the cells were viable with spread morphology in the hydrogel matrix (Fig. 3B and S5, Supporting Information). Based on these results, the 2-HA-Col hydrogel was selected as the carrier for cell delivery.

SEM

The 2-HA-Col hydrogel had a porous microstructure with an average pore size of $74.4 \pm 10.0 \mu\text{m}$ (Fig. 3C). The attachment of ADSCs on the 2-HA-Col hydrogel was also observed by SEM. They exhibited an elongated morphology in the hydrogel matrix, which was consistent with the finding of 3D culture (Fig. 3D).

Cell-protective effect of the 2-HA-Col hydrogel

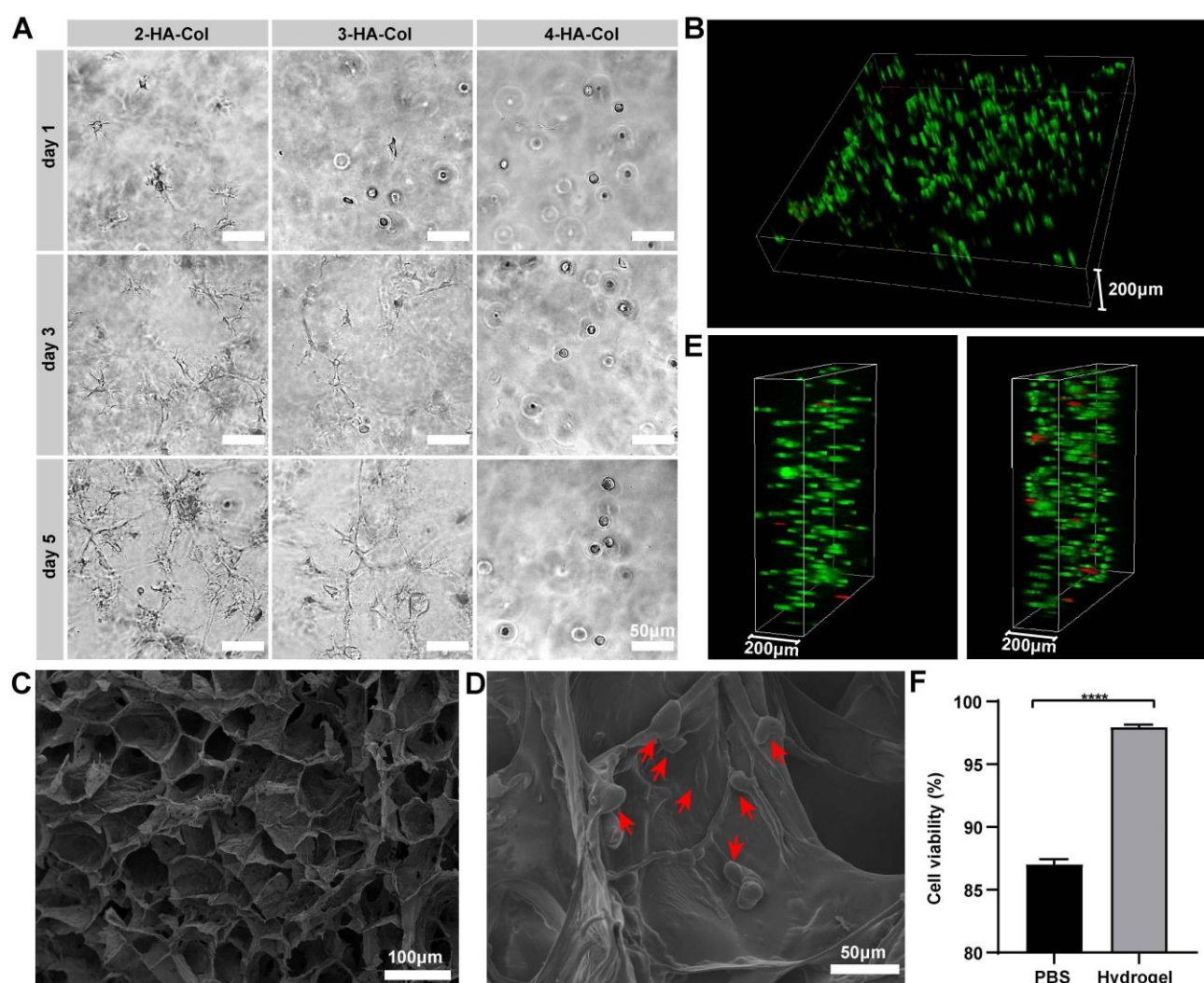


Fig. 3 Evaluation of the cytocompatibility and protective potential of HA-Col hydrogel. A) Morphology of ADSCs encapsulated in different hydrogel formulations on days 1, 3, and 5 of cell culture. B) Live/dead staining images of ADSCs encapsulated in 2-HA-Col after 3 days of 3D culture, where Calcein AM stained live cells green and PI stained dead cells red. C) SEM image of 2-HA-Col hydrogel. D) SEM image indicated the cell morphology (red arrows) when encapsulated in 2-HA-Col hydrogel after 1 day of 3D culture. E) Live/dead staining images of ADSCs 1 h post-injection within 2-HA-Col (left) and PBS (right). The injection was performed through a 25-gauge needle with an inner diameter of 0.5 mm. F) Quantification of the viability of ADSCs in PBS and 2-HA-Col hydrogel 1 h post-injection. Data are presented as the mean \pm standard deviation ($n = 3$), **** $p < 0.0001$.

The cell-hydrogel construct was injected through a 25-gauge needle and performed with live/dead staining 1 h post-injection. As shown in Fig. 3E, the injection of ADSCs within 2-HA-Col hydrogel led to obviously fewer cell death than the injection of cell-PBS suspension. Specifically, more than 97% of the cells remained alive when administered using the hydrogel as cell carrier (Fig. 3F).

Preparation and characterization of T-ADSCs

Different PBAE/pEGFP-TGF- β 1 nanocomplex formulations were prepared and characterized (Fig. S6, Supporting Information). The PBAE/pEGFP-TGF- β 1 nanocomplex formulated at a weight ratio of 60/1 was selected as the gene transfection agent for the preparation of T-ADSCs considering both transfection efficiency and cell toxicity (Fig. S7, Supporting Information). The long-lasting expression of EGFP was exhilaratingly observed in T-ADSCs. The proportion of EGFP positive cells peaked at 52.8% 48 h post-transfection, after which it started to decrease, leading to the decline in the EGFP fluorescence intensity (Fig. 4A

and 4B). Noteworthy, 20% of the cells were still EGFP positive even 5 days post-transfection.

Meanwhile, the ADSCs were able to continually express TGF- β 1 after transfection. The cumulative expression of TGF- β 1 in T-ADSCs was 34.3% higher than that of the non-transfected ADSCs even 5 days post-transfection (Fig. 4C). Obvious toxicity was not observed during 5 days of transfection via cell proliferation test, which indicated the excellent cytocompatibility of the optimal PBAE/pEGFP-TGF- β 1 nanocomplexes (Fig. 4D).

The enhanced paracrine effect on OA-like chondrocytes of T-ADSCs

Chondrocytes were isolated from the knee joint of the rat. As shown in Fig. S8, the isolated cells formed stretched, polygonal-shaped pseudopodia after culture and expressed the typical biomarker of chondrocytes, Col II.

The chondrocytes were co-culture with ADSCs, or T-ADSCs in transwells for 3 days, followed by the extract of the total RNA of chondrocytes in wells for qRT-PCR analysis (Fig. 4E). As shown

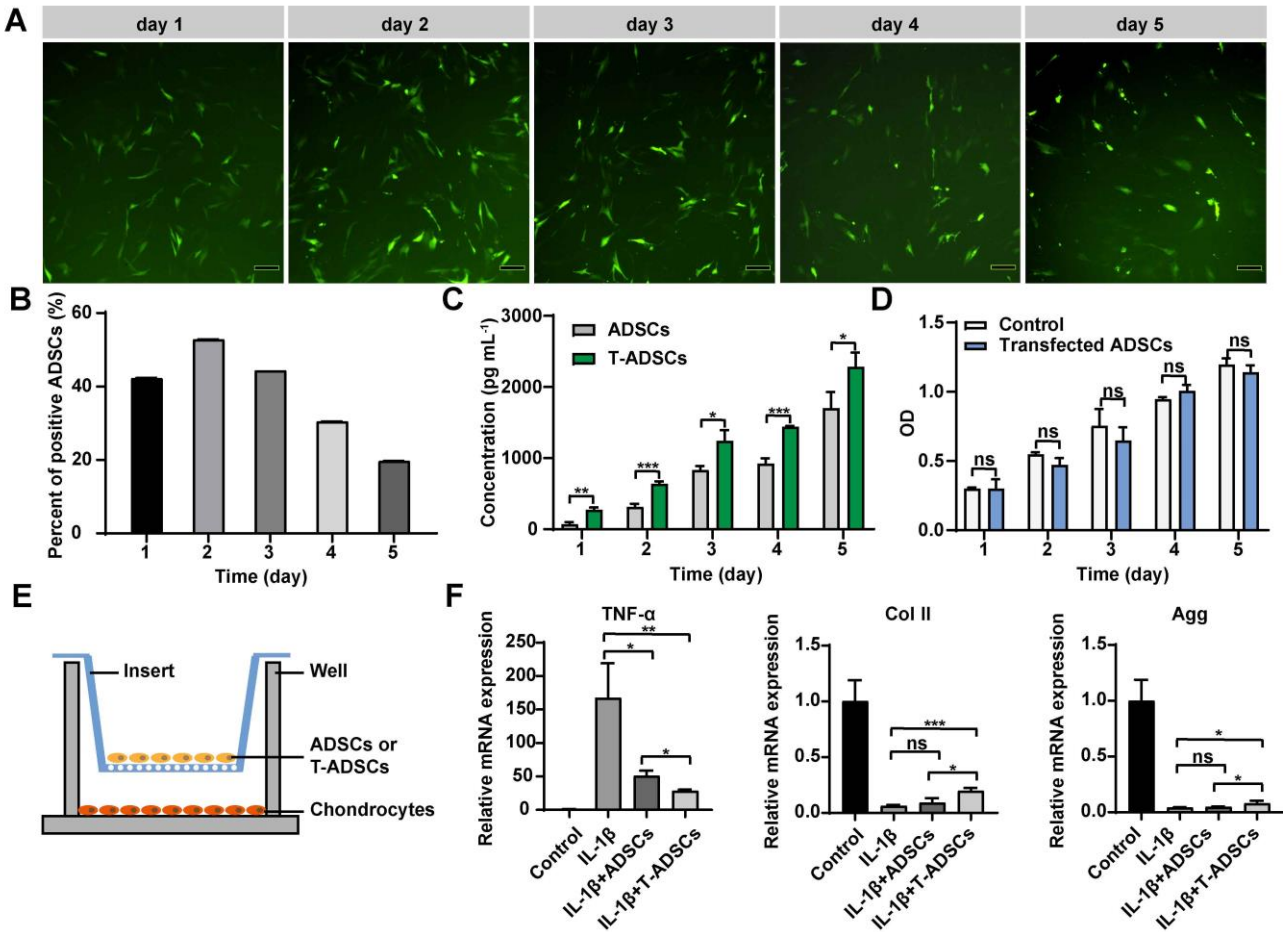


Fig. 4 Transfection of ADSCs and co-culture experiment. A) EGFP expression in ADSCs transfected with PBAE/pEGFP-TGF- β 1 nanocomplexes at a weight ratio of 60/1 lasted over time. Scale bar 200 μ m. B) Percentage of EGFP positive cells evaluated by flow cytometry. $n = 3$. C) Cumulative concentrations of TGF- β 1 in ADSCs and T-ADSCs groups at different time points determined by ELISA. $n = 3$, * $p < 0.05$, ** $p < 0.01$, *** $p < 0.001$. D) Cell proliferation test of ADSCs transfected with PBAE/pEGFP-TGF- β 1 nanocomplexes at a weight ratio of 60/1, non-transfected ADSCs were used as control. $n = 3$, ns represents $p > 0.05$. E) The schematic illustration of the co-culture system. The insert contains chondrocytes, ADSCs or T-ADSCs, and the well contains chondrocytes. F) qRT-PCR analysis of total RNA extracted from the chondrocytes in the wells on day 3 of co-culture. $n = 3$, * $p < 0.05$, ** $p < 0.01$, *** $p < 0.001$. Data are presented as the mean \pm standard deviation ($n = 3$).

in Fig. 4F, the addition of IL-1 β resulted in a significant decrease in the levels of Col II and aggrecan (Agg) mRNA by 94.0% and

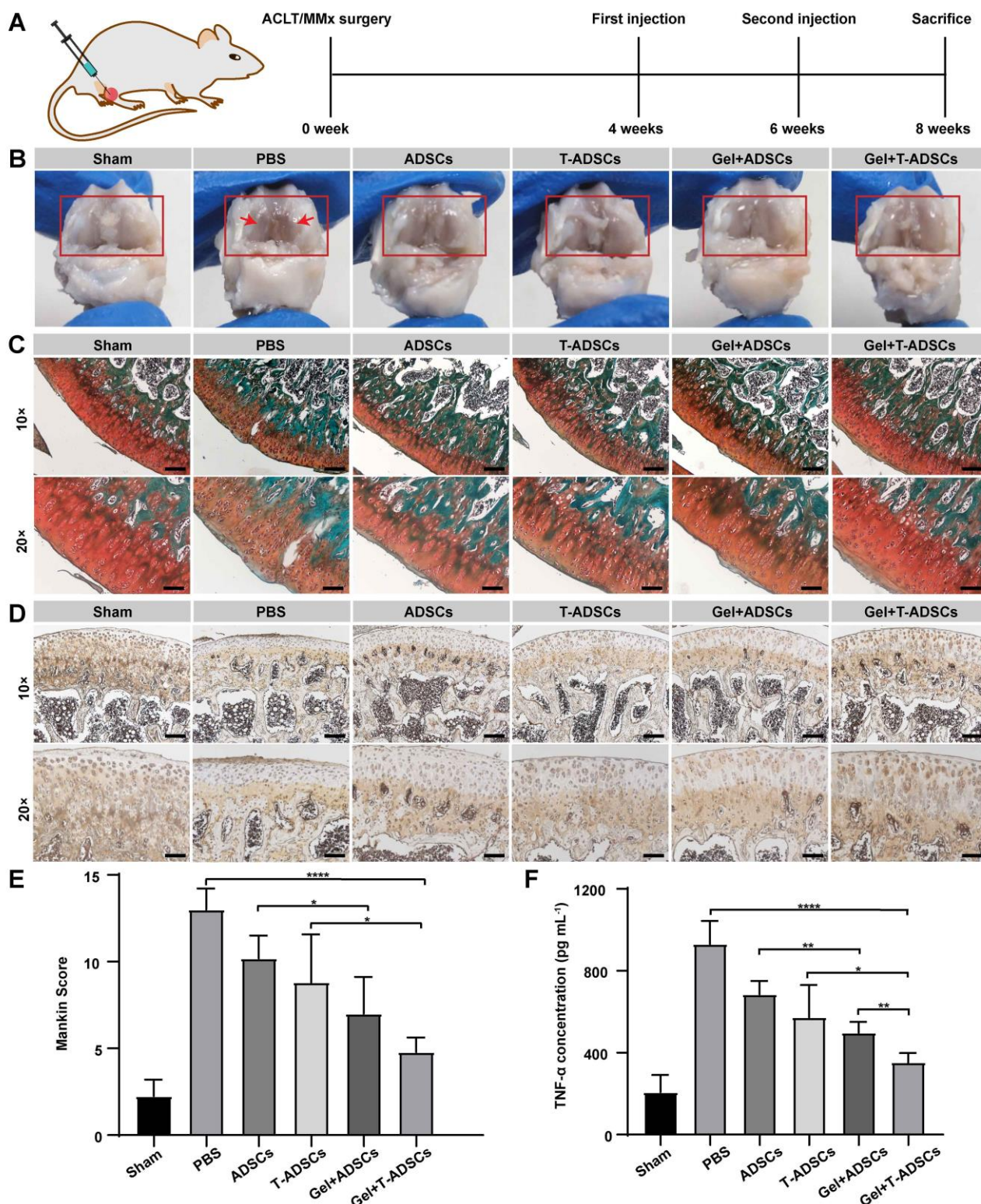


Fig. 5 Macroscopic and histological examination. A) Graphical representation of the animal experimental design. B) The gross appearance of the femurs (red frames). Red arrow denotes cartilage degeneration. Histological analysis through C) Safranin O/Fast Green staining and D) immunohistochemical staining of Col II. Scale bar of 10 \times images: 200 μ m; Scale bar of 20 \times images: 100 μ m. E) Mankin scores of tissue cross-sections. $n = 5$, * $p < 0.05$, **** $p < 0.0001$. F) The concentration of TNF- α in synovial fluid collected from different treatment groups. $n = 5$, * $p < 0.05$, ** $p < 0.01$, **** $p < 0.0001$. Data are presented as the mean \pm standard deviation ($n = 5$).

96.0% respectively, and an increase by 166.3 folds in the level of TNF- α mRNA compared to that of the control group (without the addition of IL-1 β). The levels of Col II and Agg mRNA showed no statistical significance between IL-1 β +ADSCs group and IL-1 β group. However, mRNA levels of Col II and Agg were 3.268 folds and 1.934 folds higher in the IL-1 β +T-ADSCs group than in the IL-1 β group, respectively, indicating that ADSCs were imparted with the enhanced paracrine effects following gene modification. Besides, the TNF- α mRNA level was downregulated by 83.06% and 69.56% in the IL-1 β +T-ADSCs and IL-1 β +ADSCs groups, respectively, which highlighted the enhanced therapeutic effects of T-ADSCs.

Chondroprotective effect of T-ADSCs-loaded hydrogel

The rat OA model was established by ACLT/MMx surgery (Fig. S9, Supporting Information). PBS, ADSCs, T-ADSCs, ADSCs-loaded hydrogel, or T-ADSCs-loaded hydrogel were injected into the affected joint of the rats 4 and 6 weeks post-surgery (Fig. 5A). By analyzing the gross appearance of the femurs, the cartilage was found to be eroded and worn out (red frame) following PBS treatment, showing the typical degenerative changes of OA (Fig. 5B). Compared with PBS control group, these symptoms were alleviated after treatment with ADSCs, T-ADSCs, ADSCs-loaded hydrogel, or T-ADSCs-loaded hydrogel. The Safranin O/Fast Green staining revealed the decrease in proteoglycans (red) content in the PBS group (Fig. 5C). But alleviated degenerative feature was observed in the cells or cells-loaded hydrogel treatment groups. Higher content of proteoglycans was also generated in these groups, where the Gel+T-ADSCs group displayed the highest level of proteoglycans. Col II, an important indicator of ECM protein,³⁸ was significantly decreased in its expression in the PBS group (Fig. 5D). Interestingly, the group treated with T-ADSCs-loaded hydrogel presented much stronger signal of Col II than other groups in both the superficial and middle areas, exerting the best chondroprotective effect among tested groups. As shown in Fig. 5E, compared to PBS group, the other treatment groups demonstrated lower Mankin scores of articular cartilage. After hydrogel encapsulation, reduced Mankin scores were observed in Gel+ADSCs and Gel+T-ADSCs treatment group. T-ADSCs-loaded hydrogel treatment resulted in the lowest Mankin score, highlighting its promising chondroprotective effect.

Anti-inflammatory effect of T-ADSCs-loaded hydrogel

As shown in Fig. 5F, the PBS group led to the presence of the highest amount of TNF- α in synovial fluid. Treatment with cell or cell-loaded hydrogels decreased the production of TNF- α . Compared to the unmodified ADSCs group, the T-ADSCs enhanced the cellular function of anti-inflammation as evidenced by lower TNF- α production in synovial fluid. Among all the treatment groups, the Gel+T-ADSCs group showed the strongest anti-inflammatory effect, which significantly downregulated TNF- α level by 62.1% compared to the PBS control. The H&E staining of synovial joint tissue revealed that

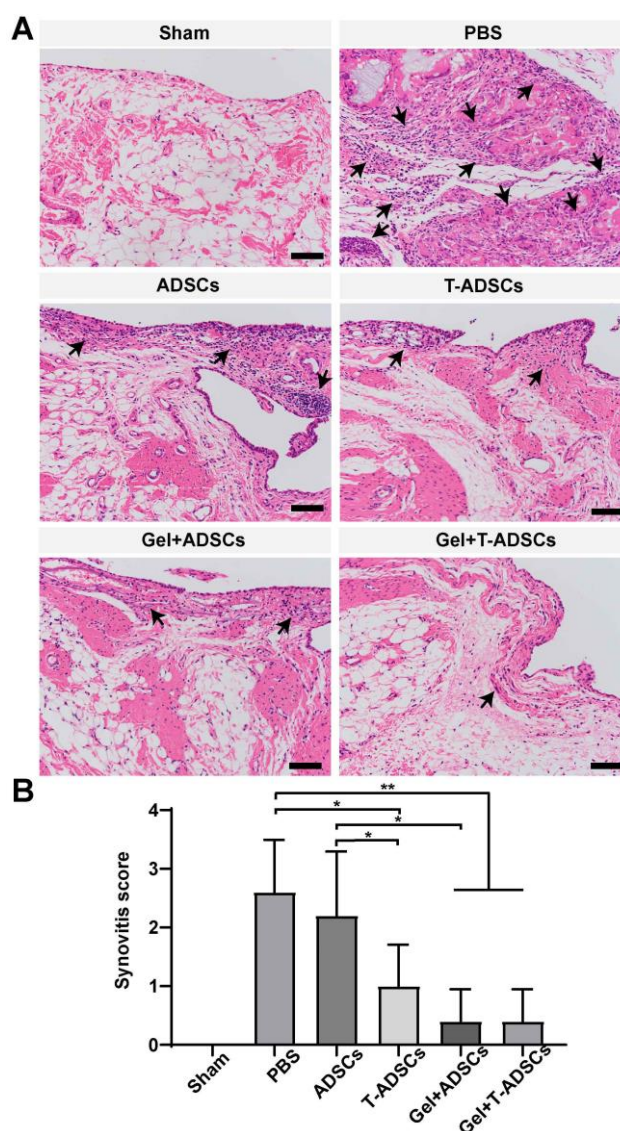


Fig. 6 Evaluation of synovitis. A) H&E staining of synovial joint tissue. Black arrows denote inflammatory cells. Scale bar 100 μ m. B) Synovitis scores of different groups based on the semi-quantitative evaluation of the three determining features of chronic synovitis: inflammatory infiltrate, synovial stroma and lining cell hyperplasia. Data are presented as the mean \pm standard deviation ($n = 5$), * $p < 0.05$, ** $p < 0.01$.

there were fewer inflammatory cells in Gel+T-ADSCs group (Fig. 6A), while obvious infiltration of inflammatory cells was observed in the synovial joint tissue samples of PBS control group. Fig. 6B showed that treatment with T-ADSCs, Gel+ADSCs, or Gel+T-ADSCs resulted in significantly reduced synovitis scores compared with PBS control group. In comparison with the unmodified ADSCs, T-ADSCs and Gel+ADSCs treatment group exhibited a lower synovitis score, suggesting an improved anti-inflammatory effect.

Micro-CT

Severe bone erosion and cyst (red arrows) were observed in the PBS group after 4 weeks of treatment, whereas the cells or cells-

loaded hydrogel groups showed mild to moderate degree of bone erosion, loss, and cyst (Fig. 7A and 7B). ROI was selected to analyze the trabecular bone microstructure (Fig. 7C). An evident bone loss was generated in the PBS group. Compared to the sham group, the bone volume/tissue volume (BV/TV) of the tibiae and femurs in the PBS group decreased by 38.2% and 17.2%, respectively, and the trabecular number (Tb. N) decreased by 26.4% and 29.6% (Fig. 7D and 7E). However, after cells or cells-loaded hydrogel treatment, bone loss was relieved.

The tibial BV/TV of Gel+T-ADSCs group was significantly higher than that of any other treatment group. The tibial and femoral Tb. N of Gel+T-ADSCs group was 28.6% and 42.1% higher than that of the PBS group, which was also higher than that of other treatment groups. Taken together, the Gel+T-ADSCs group exhibited the best therapeutic efficacy in preventing subchondral bone loss and structural destruction caused by ACLT/MMx surgery.

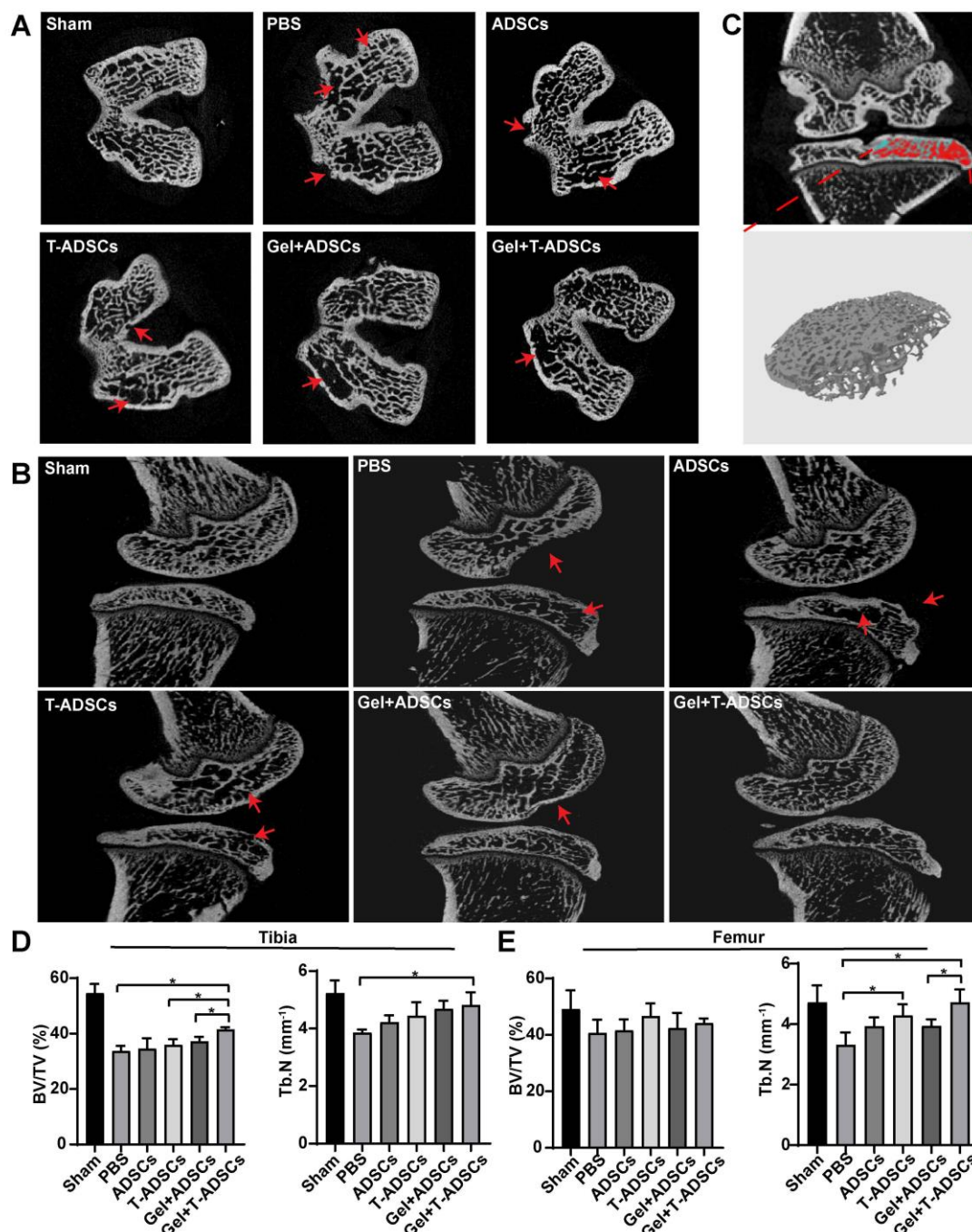


Fig. 7 Micro-CT analysis of different treatment groups. A) Representative images of femoral axial section of different treatment groups. B) Representative images of sagittal sections of the whole knee joint of different treatment groups. Red arrows denote bone erosion, loss, and cyst. C) Representative images ROI used for analysis of trabecular bone microstructure. D, E) The BV/TV and Tb. N of trabecular bone. Data are presented as the mean \pm standard deviation ($n = 3$), * $p < 0.05$.

Discussion

The intra-articular delivery of ADSCs is a promising therapy for OA treatment. Moreover, the therapeutic effects could be further enhanced by genetic modification of ADSCs to overexpress TGF- β 1. Consequently, the direct injection of ADSCs leads to mechanical damage and poor retention of therapeutic cells.³⁹ Recently, ECM-mimicking hydrogels have shown enormous potential in cell-mediated tissue regeneration, including cartilage and muscle regeneration.^{40, 41} Herein, we delivered gene-engineered ADSCs within an ECM-mimicking hydrogel, which exhibited improved therapeutic outcomes of ADSCs for OA treatment.

HA, a linear polysaccharide consisting of alternating units of glucuronate and *N*-acetylglucosamine, is the main component of ECM in many tissues including cartilage, synovial and connective tissue.⁴² HA restores the viscoelastic property of synovial fluid and protects chondrocytes from apoptosis.^{43, 44} However, it lacks the ability to support cell adhesion.⁴⁵ As a major structural component of many tissues, Col I is able to self-assemble into collagen fibers in the physiological environment and provides cells with adhesion sites.⁴⁵ Thus, the incorporation of Col I into HA-based injectable hydrogel simulates the ECM environment, serving as an ideal carrier for the intra-articular delivery of therapeutic cells. In the present study, we prepared an ECM-mimicking hydrogel via the self-crosslink of HA-SH and self-assembly of Col I, which can be enzymatically or chemically degraded by reductants secreted in the physiological environment such as glutathione.⁴⁶⁻⁴⁸ The hydrogel could be formed *in situ* under physiological conditions, and the formation of disulfide bond and fibrillogenesis of Col I was accelerated when the pH of the precursor solution was slightly increased to 7.8.^{49, 50} The hydrogel precursor turned into a gel state within 6 minutes, allowing for the homogeneous encapsulation of ADSCs in the hydrogel without aggregation.⁵¹

The stiffness of the hydrogel is crucial for ADSCs survival and growth, and the hydrogel matrix with a stiffness similar to the native microenvironment is favorable. Therefore, hydrogels with different stiffnesses were screened in the 3D culture study of ADSCs which were encapsulated within the hydrogel matrix to evaluate the cytocompatibility. The 4-HA-Col matrix with the highest stiffness (over 1 kPa) among the candidate hydrogels resulted in the unchanged round morphology of ADSCs during the culture period. However, the cells exhibited elongated, well-spread, and interconnected morphology when cultured in the relatively softer 2-HA-Col hydrogel. Additionally, 2-HA-Col exhibited shear-thinning property, which enabled the cell delivery through the minimally invasive approach of injection,⁵² while maintained cell viability of up to 97% during this process. Taken all together, the 2-HA-Col hydrogel was selected as the carrier for the intra-articular delivery of ADSCs.

For the genetic engineering of ADSCs, the optimal nanocomplex formulation was screened and identified, which exhibited a favorable transfection efficiency and cytocompatibility on ADSCs. Meanwhile, the constant and increased expression of TGF- β 1 lasting up to 5 days was detected in T-ADSCs. These results indicated that gene

modification with the optimal PBAE/pEGFP-TGF- β 1 nanocomplexes endowed ADSCs with enhanced paracrine effects.

To investigate the impact of T-ADSCs on OA-like chondrocytes, a co-culture system was established to mimic the *in vivo* interaction between therapeutic cells and OA-like chondrocytes. The production of catabolic factors in the OA microenvironment could be upregulated by pro-inflammatory cytokines, including TNF- α and IL-1 β secreted by chondrocytes, synovial tissues, mononuclear, and osteoblast, which leads to the degeneration of cartilage and synovitis.^{53, 54} Therefore, the level of proinflammatory cytokines secreted by OA-like chondrocytes was evaluated. Consistent with the results reported in a previous study, the treatment of ADSCs decreased the expression of TNF- α in OA-like chondrocytes.³⁶ As expected, a significantly more potent anti-inflammatory effect was observed following the treatment of T-ADSCs than ADSCs. This could be attributed to the enhanced expression of TGF- β 1 that effectively alleviated the proinflammatory state of OA-like chondrocytes resulted from IL-1 β stimulation.⁵⁵ Please note that the *in vitro* experiments were performed in triplicate, which might be a limitation for statistical evaluation. We will further increase the number of replicates to validate the statistical significance during future preclinical development.

Finally, the *in vivo* therapeutic effect of ECM-mimicking hydrogel carrying T-ADSCs was evaluated on a surgically induced rat OA model which has been commonly used in OA research. A previous study demonstrated that ADSCs could decrease the TNF- α production in synovial fluid, thereby reducing joint inflammation.⁵⁶ Herein, the content of TNF- α in synovial fluid was quantified to evaluate the *in vivo* anti-inflammatory effect of different treatment groups. A lower expression of TNF- α was detected in T-ADSCs group than in ADSCs group, and encapsulation of ADSCs or T-ADSCs within the hydrogel further inhibited TNF- α production. The optimal anti-inflammatory effect of Gel+ADSCs treatment was validated by the lowest expression of TNF- α in synovial fluid. The histological examination revealed the highest content of proteoglycans and Col II in the cartilage following the treatment of T-ADSCs-loaded hydrogel, highlighting its potential protective effects on cartilage. Meanwhile, the remarkable chondroprotective and anti-inflammatory effects following T-ADSCs-loaded hydrogel treatment in turn contributed to the reduction on subchondral bone loss and destruction. The favorable therapeutic benefits from T-ADSCs-loaded hydrogel were likely attributed to the following aspects: 1) the ECM-mimicking hydrogel provided desirable structural support and protection for cells during and post-implantation, thereby maintaining the cell viability; 2) the gene-engineered ADSCs that overexpressed TGF- β 1 were endowed with the enhanced the paracrine chondroprotective effects by increasing the expression of the ECM proteins and decreasing the production of proinflammatory cytokines, which improved the therapeutic efficacy.

Conclusions

In summary, we successfully developed an ECM-mimicking hydrogel incorporating the gene-engineered ADSCs, and investigated its potent therapeutic effects for OA treatment. The yielded injectable hydrogel served as an ideal carrier for cell delivery with excellent cytocompatibility and protective effect. Meanwhile, ADSCs were successfully engineered to overexpress TGF- β 1 through nanocomplex-mediated transfection, and the resulted T-ADSCs showed an enhanced paracrine effect on OA-like chondrocytes. In a surgically induced rat OA model, the intra-articular injection of the T-ADSCs-loaded hydrogel significantly alleviated cartilage degeneration, joint inflammation, subchondral bone loss, and structure destruction. Overall, this study provides a promising strategy to synergistically improve the therapeutic effects of ADSCs for OA treatment by delivering genetically modified ADSCs that overexpress TGF- β 1 within an ECM-mimicking hydrogel.

Author Contributions

Wei Yu: Methodology, Investigation, Data analysis, Writing - original draft. Bin Hu: Writing - original draft, Methodology. Kofi Oti Boakye-Yiadom: Writing - original draft, Investigation. William Ho: Methodology. Qijing Chen: Methodology. Xiaoyang Xu: Conceptualization, Supervision, Funding acquisition, Methodology, Writing - review & editing. Xue-Qing Zhang: Conceptualization, Supervision, Funding acquisition, Methodology, Writing - review & editing. All authors have given approval to the final version of the manuscript.

Conflicts of interest

There are no conflicts to declare.

Acknowledgements

X.Zhang acknowledges the financial support from the Interdisciplinary Program of Shanghai Jiao Tong University (project number ZH2018ZDA36 (19X190020006)), Shanghai Jiao Tong University Scientific and Technological Innovation Funds (2019TPA10), and the Foundation of National Facility for Translational Medicine (Shanghai) (TMSK-2020-008). X.X. acknowledges the support from American Heart Association (19AIREA34380849) and the National Science Foundation (2001606).

References

1. Y. Liu, A. Jackson and S. Cosgrove, *Osteoarthritis Cartilage*, 2009, **17**, 1333-1340.
2. K. Sinusas, *Am. Fam. Physician*, 2012, **85**, 49-56.
3. A. D. Woolf and B. Pfleger, *Bull. World Health Organ.*, 2003, **81**, 646-656.
4. R. Liu-Bryan and R. Terkeltaub, *Nat. Rev. Rheumatol.*, 2015, **11**, 35-44.
5. M. Bhattacharjee, J. L. E. Ivirico, H.-M. Kan, R. Bordett, R. Pandey, T. Otsuka, L. S. Nair and C. T. Laurencin, *Sci. Rep.*, 2020, **10**, 1-15.
6. L.-B. Jiang, S. Lee, Y. Wang, Q.-T. Xu, D.-H. Meng and J. Zhang, *Osteoarthritis Cartilage*, 2016, **24**, 1071-1081.
7. C. Manferdini, M. Maumus, E. Gabusi, A. Piacentini, G. Filardo, J. A. Peyrafitte, C. Jorgensen, P. Bourin, S. Fleury - Cappellesso and A. Facchini, *Arthritis Rheum.*, 2013, **65**, 1271-1281.
8. M. Maumus, C. Manferdini, K. Toupet, J.-A. Peyrafitte, R. Ferreira, A. Facchini, E. Gabusi, P. Bourin, C. Jorgensen and G. Lisignoli, *Stem Cell Res.*, 2013, **11**, 834-844.
9. H. Jung, H. H. Kim, D. H. Lee, Y.-S. Hwang, H.-C. Yang and J.-C. Park, *Cytotechnology*, 2011, **63**, 57-66.
10. E. D. Ahmadi, T. I. Raja, S. A. Khaghani, C. F. Soon, M. Mozafari, M. Youseffi and F. Sefat, *Materials Today: Proceedings*, 2018, **5**, 15540-15549.
11. E. B. Davidson, P. Van der Kraan and W. Van Den Berg, *Osteoarthritis Cartilage*, 2007, **15**, 597-604.
12. H. Lee, H. Kim, J. Seo, K. Choi, Y. Lee, K. Park, S. Kim, A. Mobasheri and H. Choi, *Inflammopharmacology*, 2020, **28**, 1237-1252.
13. E. A. Silva, E.-S. Kim, H. J. Kong and D. J. Mooney, *Proc. Natl. Acad. Sci. U. S. A.*, 2008, **105**, 14347-14352.
14. Y. Wang, X. He, K. F. Bruggeman, B. Gayen, A. Tricoli, W. M. Lee, R. J. Williams and D. R. Nisbet, *Adv. Funct. Mater.*, 2020, **30**, 1900390.
15. Z. Tang, F. Jiang, Y. Zhang, Y. Zhang, X. Huang, Y. Wang, D. Zhang, N. Ni, F. Liu and M. Luo, *Biomaterials*, 2019, **194**, 57-72.
16. M. W. Tibbitt and K. S. Anseth, *Biotechnol. Bioeng.*, 2009, **103**, 655-663.
17. K. T. Nguyen and J. L. West, *Biomaterials*, 2002, **23**, 4307-4314.
18. A. P. Mathew, S. Uthaman, K.-H. Cho, C.-S. Cho and I.-K. Park, *Int. J. Biol. Macromol.*, 2018, **110**, 17-29.
19. J. Wu, Q. Chen, C. Deng, B. Xu, Z. Zhang, Y. Yang and T. Lu, *Theranostics*, 2020, **10**, 9843-9864.
20. H. Zhou, C. Liang, Z. Wei, Y. Bai, S. B. Bhaduri, T. J. Webster, L. Bian and L. Yang, *Mater. Today*, 2019, **28**, 81-97.
21. Z. Yuan, Y.-H. Tsou, X.-Q. Zhang, S. Huang, Y. Yang, M. Gao, W. Ho, Q. Zhao, X. Ye and X. Xu, *ACS Appl. Mater. Interfaces*, 2019, **11**, 38429-38439.
22. Y. Dong, A. O. Saeed, W. Hassan, C. Keigher, Y. Zheng, H. Tai, A. Pandit and W. Wang, *Macromol. Rapid Commun.*, 2012, **33**, 120-126.
23. B. A. Bunnell, M. Flaatt, C. Gagliardi, B. Patel and C. Ripoll, *Methods*, 2008, **45**, 115-120.
24. C. Lorenzo, G. Pérez-Chacón, G. Garaulet, Z. Mallorquín, J. M. Zapata and A. Rodríguez, *Cancer Gene Ther.*, 2015, **22**, 542-551.
25. T. T. Smith, S. B. Stephan, H. F. Moffett, L. E. McKnight, W. Ji, D. Reiman, E. Bonagofski, M. E. Wohlfahrt, S. P. Pillai and M. T. Stephan, *Nat. Nanotechnol.*, 2017, **12**, 813-820.
26. K. Chen, Y. Yan, C. Li, J. Yuan, F. Wang, P. Huang, N. Qian, J. Qi, H. Zhou and Q. Zhou, *Cell Death Dis.*, 2017, **8**, e3109-e3109.
27. Z. Qiao, J. Tang, W. Wu, J. Tang and M. Liu, *BMC Complement. Altern. Med.*, 2019, **19**, 1-8.
28. Y. Shi, X. Hu, J. Cheng, X. Zhang, F. Zhao, W. Shi, B. Ren, H. Yu, P. Yang and Z. Li, *Nat. Commun.*, 2019, **10**, 1-14.
29. T. Hayami, M. Pickarski, Y. Zhuo, G. A. Wesolowski, G. A. Rodan and L. T. Duong, *Bone*, 2006, **38**, 234-243.
30. H. R. Moody, B. J. Heard, C. B. Frank, N. G. Shrive and A. O. Oloyede, *J. Anat.*, 2012, **221**, 47-54.
31. V. Krenn, L. Morawietz, T. Häupl, J. Neidel, I. Petersen and A. König, *Pathol. Res. Pract.*, 2002, **198**, 317-325.
32. Y. Chen, J. Sui, Q. Wang, Y. Yin, J. Liu, Q. Wang, X. Han, Y. Sun, Y. Fan and X. Zhang, *Carbohydr. Polym.*, 2018, **190**, 57-66.

33. G. L. Ellman, K. D. Courtney, V. Andres Jr and R. M. Featherstone, *Biochem. Pharmacol.*, 1961, **7**, 88-95.
34. X. Z. Shu, Y. Liu, Y. Luo, M. C. Roberts and G. D. Prestwich, *Biomacromolecules*, 2002, **3**, 1304-1311.
35. M. Guvendiren, H. D. Lu and J. A. Burdick, *Soft Matter*, 2012, **8**, 260-272.
36. L. Mei, B. Shen, P. Ling, S. Liu, J. Xue, F. Liu, H. Shao, J. Chen, A. Ma and X. Liu, *PLoS One*, 2017, **12**, e0176107.
37. A. Schäffler and C. Büchler, *Stem Cells*, 2007, **25**, 818-827.
38. Y. Xu, Y. Gu, F. Cai, K. Xi, T. Xin, J. Tang, L. Wu, Z. Wang, F. Wang and L. Deng, *Adv. Funct. Mater.*, 2020, **30**, 2006333.
39. L. Cai, R. E. Dewi and S. C. Heilshorn, *Adv. Funct. Mater.*, 2015, **25**, 1344-1351.
40. Y. Yao, P. Wang, X. Li, Y. Xu, G. Lu, Q. Jiang, Y. Sun, Y. Fan and X. Zhang, *Acta Biomater.*, 2020, **111**, 197-207.
41. Y. Xu, X. Chen, Y. Qian, H. Tang, J. Song, X. Qu, B. Yue and W. E. Yuan, *Adv. Funct. Mater.*, 2020, **30**, 2002378.
42. M. Shafiq, Y. Jung and S. H. Kim, *Biomaterials*, 2016, **90**, 85-115.
43. R. D. Altman, A. Manjoo, A. Fierlinger, F. Niazi and M. Nicholls, *BMC Musculoskelet. Disord.*, 2015, **16**, 1-10.
44. P. Wehling, C. Evans, J. Wehling and W. Maixner, *Ther. Adv. Musculoskelet. Dis.*, 2017, **9**, 183-196.
45. S. R. Caliarì and J. A. Burdick, *Nat. Methods*, 2016, **13**, 405-414.
46. M. Kar, Y.-R. V. Shih, D. O. Velez, P. Cabrales and S. Varghese, *Biomaterials*, 2016, **77**, 186-197.
47. S.-Y. Choh, D. Cross and C. Wang, *Biomacromolecules*, 2011, **12**, 1126-1136.
48. J. Zhang, A. Skardal and G. D. Prestwich, *Biomaterials*, 2008, **29**, 4521-4531.
49. D. Bermejo-Velasco, A. Azémar, O. P. Oommen, J. n. Hilborn and O. P. Varghese, *Biomacromolecules*, 2019, **20**, 1412-1420.
50. T. Walimbe, S. Calve, A. Panitch and M. P. Sivasankar, *Acta Biomater.*, 2019, **87**, 97-107.
51. K. Gwon, E. Kim and G. Tae, *Acta Biomater.*, 2017, **49**, 284-295.
52. H. Wang, D. Zhu, A. Paul, L. Cai, A. Enejder, F. Yang and S. C. Heilshorn, *Adv. Funct. Mater.*, 2017, **27**, 1605609.
53. M. Kapoor, J. Martel-Pelletier, D. Lajeunesse, J.-P. Pelletier and H. Fahmi, *Nat. Rev. Rheumatol.*, 2011, **7**, 33-42.
54. R. Liu-Bryan, *Curr. Rheumatol. Rep.*, 2013, **15**, 323.
55. H. Van Beuningen, P. Van der Kraan, v. d. O. Arntz and W. Van Den Berg, *Ann. Rheum. Dis.*, 1993, **52**, 185-191.
56. L. Mei, B. Shen, J. Xue, S. Liu, A. Ma, F. Liu, H. Shao, J. Chen, Q. Chen and F. Liu, *Biochem. Biophys. Res. Commun.*, 2017, **494**, 285-291.